This is a repository copy of *Histopathology in 3D: from three-dimensional reconstruction to multi-stain and multi-modal analysis*.

Article:

Histopathology in 3D: From 3D Reconstruction to Multi-stain and Multi-modal Analysis

Abstract

Light Microscopy applied to the domain of histopathology has traditionally been a two dimensional imaging modality. Several authors, including the authors of this work, have extended the use of Digital Microscopy to three dimensions by stacking digital images of serial sections using image based registration. In this paper we give an overview of our approach, and of extensions to the approach to register multi-modal data sets such as sets of interleaved histopathology sections with different stains, and sets of histopathology images to Radiology volumes with very different appearance. Our approach involves transforming dissimilar images into a multi-channel representation derived from co-occurrence statistics between roughly aligned images.

1. Introduction

A number of authors have addressed the problem of reconstruction of volumetric data from serial histopathology sections. These approaches may divided into those approaches that rely on the tissue only (e.g. [11]), and those that use a form of 3D imaging (radiology, or blockface imaging) to aid the reconstruction (e.g. [10,12]). Within both groups image based registration is usually based on either an iterative optimisation of a similarity metric [13], or feature detection and matching [5]. Either approach has drawbacks. Optimisation based approaches can find local optima of the similarity function. With volumetric reconstruction it is necessary to either perform a large number of registrations (one per section) (e.g. [5]), or optimisation in a very high dimensional space [13], either increasing the likelihood of failure. With feature detection based methods the features must be appropriate to the data, and thus a truly generic method is not possible. We have previously presented an alternative approach based on combining multiple local rigid registrations into a single non-rigid transform using a robust statistical estimator [1]. We use a closed form method of rigid registration based on Phase Correlation [14,15] to perform local rigid registration. This was selected as it is computationally efficient (four Fourier transforms, and a fixed set of multiplies and adds), and is guaranteed to find the maxima of similarity as it is equivalent to an exhaustive search. The drawback of this method when applied to multi-modal data is that it is based on greyscale similarity. The conventional approach to multi-modal registration is to use mutual information as a similarity metric [6]. However, this implies an iterative method – with associated computational complexity and risk of local optima. Our alternative approach is to transform pairs of multi-modal images into pairs of multi-channel "tissue class

probability" images based on co-occurrence statistics of roughly aligned images. Mutual Information is used within the process of forming these emergent tissue classes from the image pair (a rather different use of MI than the conventional similarity metric in registration). Once the multi-channel tissue class probability images have been formed, registration proceeds as with the single stain registration, excepting for the fact that there are N sets of local registrations (one per emergent tissue class). These are combined as before within our multi-level robust statistics framework to form a single B-spline based registration. The remainder of this paper is as follows: Section 2 details the basic robust statistical framework used in both the single-stain and Multi-modal registrations; Section 3 details the formation of the multi-channel "tissue class probability" images from roughly aligned images; Section 4 presents some case studies of applications of the technology; and Section 5 presents a discussion and conclusion.

2. Volumetric Reconstruction from Serial Sections Using Robust Statistics

The main idea behind our method is that a single non-rigid registration for a pair of large images may be performed as a set of rigid registrations on sub-images, which are subsequently combined. This has the dual advantage of computational efficiency (memory and processor usage) and robustness (a single registration failure is not catastrophic as there is redundancy). In order to implement this idea, images are and padded to the same size and pre-aligned rigidly, in order that (roughly) corresponding regions may be extracted by dividing the images into regular grids. The basic workflow of our robust statistical framework is:

For images n=1:N-1

1. Pad images to the same size.
2. Rigidly align images n and n+1 using Greyscale Phase Correlation (Image n=static image, image n+1=moving image)
3. Divide each image pair into equal sized 50% overlapping patches, and rigidly align corresponding patches using a form of phase correlation that recovers rotation (see [1] for details).
4. For each local registration construct 5 transform vectors (one at each corner, and one in the middle) from each registration.
5. Approximate the set of vectors by a rigid transform using a least squares minimising method, and subtract this transform from each vector.
6. Approximate the "residual transform vector" set using a B-spline using a robust least squares minimising method [2].
7. Use transformed image n+1 as static image for image n+2

In practice steps 3-6 are repeated at multiple scales (from coarse to fine) and increasing degrees of freedom of the B-spline. The reference image is selected by hand as an image with minimal distortion (to avoid propagating distortions to subsequent images). This approach has been applied successfully to reconstruct

several hundred volumes of different tissue types and chemical stains. A number of examples are visualised in Figures 1 and 3.

3. Multi-stain and Multi-modal Registration

In this section the generation of mapping functions to map images of different appearance to multi-channel images of more similar appearance is described. The outline of the method is as follows:

1. Represent each pixel of each image by a feature vector derived from local intensity, colour and texture. These features in include the output of Gaussian filters on colour and greyscale channels, and a novel derivative based texture feature (see [16] for details).
2. Quantise the set of features separately for each image such that each pixel is represented by a prototype label (L1x,y , L2x,y). Clustering is performed using a binary PCA-tree method (see [16] for details). This method was selected for its computational efficiency, and ability to work with variation of different scales.
3. Consider a pair of hypothesised mapping functions that map the prototypes to a finite set of common tissue classes:
   $C1_{x,y} = M1(L1_{x,y})$
   $C2_{x,y} = M2(L2_{x,y})$
4. For a given pair of mapping functions it is possible to generate a tissue class co-occurrence matrix. The Mutual information calculated from this matrix is a measure of the similarity between the two images under that pair of mapping functions (and that feature set). A greedy search of potential mapping functions is performed in order to maximise mutual information, and select the best mapping functions.
5. The method is repeated with different feature sub-sets in order to perform feature selection. The feature sub-set with highest mutual information is selected.

Once the mapping functions for each image have been determined the construction of probability images for each tissue class for each image is simply a matter of considering the co-occurrence of prototype labels in one image with tissue classes in the other. Counting these co-occurrences, and normalising gives P(Tissue Class|Prototype), which is mapped to a pixel value by multiplying by 255. Figure 2 illustrates results of applying this process for both multi-stain histopathology pairs and histopathology:MRI pairs. Once the images have been constructed registration is applied as described in section 2, with 5 x N_c vectors per block (where N_c is the number of tissue classes). Initial rigid alignment is using the same greyscale phase correlation method as described previously, which works on such multi-modal data (at low resolution) because of the clear distinction between foreground and background at low resolution in histopathology images. Full details may be found in [16].

Application to Volumetric Radiology Data

For multi-stain histopathology data sets the 3D correspondence (slice to slice) is explicit in the data set. For Histopathology to radiology registration a 2D oblique slice needs to be determined in order to compute tissue class probability images and subsequently perform 2D:2D non-rigid registration. Initially this is performed manually for a single histopathology image using an interactive tool (MIM Medical Image Manager, HeteroGenius Ltd, Leeds, UK http://www.heterogenius.co.uk). Once one section is aligned it's 3D location can be optimised locally by maximising mutual information between prototype labels ($MI(L1,L2)$) over a 3D rigid transform using Levenberg Marquart (LM) optimisation [17]. LM is an iterative gradient based optimisation method. Subsequent sections can be placed in 3D space with reference to their theoretical geometric relation to the initial slice(s) (i.e. parallel with known normal offset based on section thickness/separation). Again their location can be optimised by local optimisation. Once placed in 3D space registrations to slices above and below (as section 3) can be performed, in addition to registration to the volumetric radiology data. Accuracy of the method is demonstrated in figure 4b. Typically registration is accurate to within 200 microns (evaluated by measuring the distance between corresponding landmarks, such as blood vessels, in 2D), although larger deformations (such as tissue folds, and severe deformation) cannot be corrected for.

4. Case Studies

Liver Disease Quantification

We used the original volumetric reconstruction algorithm (section 2) to generate volumes from liver tissue with 5 different types of liver disease (Alcoholic Liver Disease; Hepatitis C Virus; Primary Biliary Cirrhosis; Primary Sclerosing Cholangitis and Polycystic Liver Disease) plus a healthy control (figure 3). Two $1cm^3$ tissue samples were taken for each disease and sectioned with a microtome to give approximately 100 sections per tissue sample (separation 100μm). These were stained with picro-sirius red and scanned using an Aperio T2 or T3 scanner (Aperio Inc, San Diego) at 20x objective. Figure 3 shows liver nodules (stained brown/yellow) are surrounded by patterns of fibrotic tissue (stained red). The size, shape and connectivity of nodules was quantified by i) Interactively segmenting nodules from other pixels using our in house Volume Viewer software with inplane resolution 1/64 native resolution, ii) Separating nearby nodules using a 3D sub-voxel anisotropic morphological opening procedure, and iii) assigning statistics to connected 3D components (size, elongation, etc.) using c++ code based on the Insight Toolkit (Kitware Inc., NY). The number of connected components and size of connected components showed a statistically significant variation between diseases, which is an indication of the (loss of) liver function in different diseases. Full results will be presented elsewhere.

Cardiac Collagen Quantification

The purpose of this study was to quantify the effect of sub-sampling sections on collagen quantification in rat hearts. Previous works (e.g. [7]) had used small numbers of sections (1-3) to quantify collagen density in different parts of the heart. The problem with using very sparse sections is twofold; i) Accurate identification of the cardiac regions, and ii) The collagen density is heterogeneous and, as such, sampling by taking a single section could introduce an undersampling error. To quantify the degree of the undersampling error we took 1000 5μm serial sections from each of 2 rat hearts (a male normal Wistar rat and a male Wistar rat in right heart failure) and aligned them to high resolution MRI volumes of the same hearts pre-sectioning scanned using a FLASH (Fast Low Angle SHot) MRI sequence in a Bruker (Ettlingen, Germany) 9.4T spectroscope with resolution of 50x50x50μm. Each MRI volume was manually segmented into regions as defined by a modified American Heart Association model ([8], figure 4a), which enabled labelling of each co-registered histopathology image. Collagen quantification was carried out in 2D using a standard method [9], using all 1000 sections, and also subsets of 100, 50, 10 sections. Results showed acceptable quantification down to 100 Sections (100 μm spaced sections), but thereafter sub-sampling resulted in increased variance over different data sub-sets. The lesson to be learned from this is that quantification using a single (or small numbers of) 2D section is potentially subject to sampling noise, even if the whole 2D sample is analysed. A more robust way of performing quantification is to take a larger number of samples of the tissue and aggregate the results. Full results are presented in [3].

Computational Modelling of Spinal Discs from Multiple Different Stains

Data driven computational models are a tool that can help understand disease and the implication of clinical actions (e.g. surgery). In the domain of musculoskeletal medicine physics based models (e.g. Finite Element models) may be constructed based on MRI or MicroCT data [4]. Such data only provides one value per voxel (Density in the case of MicroCT). Chemical stains used in histopathology can provide a wealth of other functional information such as collagen density (relating to elasticity), cell density, etc. However, such data is two dimensional only and, as such, not suitable for use in building 3D models. We have run experiments to reconstruct 3D data sets from multiple interleaved sections stained with different chemical stains using the methods described in section 4. Data used was from an ovine intervertebral disc. In all 5 stains were used (Alcian Blue, ERSR, FAST, Elastic Pico Sirius Red and Sirius Red) to build a multi-parametric 3D representation of the data. This volumetric data was also aligned with high resolution MRI (scanner as in previous section) to provide further anatomical information. The aim is to build multi-scale physics based models based on the anatomical and functional data provided by this rich data set. The modelling work is ongoing.

5. Discussion

Reconstructing microscopic functional and anatomical datasets in 3D using multiple 2D digital images is a powerful tool in a number of research areas including disease quantification and computational modelling. In this paper we have described how multiple sources of information (multiple chemical and immunohistochemical stains, Radiology) may be combined in a similar manner to stacking single stain 2D datasets by using an information theory based image pre-processing method. In order to facilitate such research the process of volumetric reconstruction must be as robust as possible. We have tackled this challenge using a combination of fast local analysis, robust statistics, a multi-scale approach, and a minimal (but important) amount of manual intervention. The combined method has been demonstrated to outperform iterative optimisation based techniques both in terms of accuracy, and run-time [16]. Our techniques have been applied in a number of different areas and we continue to explore applications and collaborations in surgical planning, radiology sequence development validation, disease quantification, and a number of other areas.

6. Acknowledgements

7. References

[1] Roberts N, Magee D, Song Y, Brabazon K, Shires M, Crellin D, Orsi N, Quirke P, Treanor D, Toward Routine Use of 3D Histopathology as a Research Tool, American Journal of Pathology, Vol. 180(5), 2012

[2] Tikhonov A., On the stability of inverse problems. Doklady Akademii Nauk SSSR 39 (5): 195–198, 1943

[3] Gilbert, S., Bernus, O., White E., Roberts, N., Treanor D., Magee D., A Framework for Quantification of Regional Cardiac Fibrosis from Serial Sections using 3D Whole Slide Imaging, Proc. International Conference of the IEEE Engineering in Medicine and Biology Society, 2014

[4] V. Wijayathunga, A. Jones, R. Oakland, N. Furtado, R. Hall, and R. Wilcox, "Development of specimen-specific finite element models of human vertebrae for the analysis of vertebroplasty," in Proc. Institution Mech. Eng. Part H: J. Eng. Med., 2008, vol. 222, pp. 221–228

[5] L. Cooper, K. Huang, A. Sharma, K. Mosaliganti, T. Pan, A. Trimboli, and M. Ostrowski, "Registration vs. reconstructure: Building 3d models from 2d microscopy images," in Workshop on Multi-scale Biological Imaging, 2006

[6] P. Viola P, W. Wells, H. Atsumi, S. Nakajima, R. Kikinis , Multi-modal volume registration by maximization of mutual information, Medical Image Analysis 1(1), pp 35–51,1996

[7] Correia-Pinto, J., Henriques-Coelho, T., Roncon-Albuquerque, R., Jr., Lourenco, A.P., Melo-Rocha, G., Vasques-Novoa, F., Gillebert, T.C., and Leite-Moreira, A.F.: 'Time course and mechanisms of left ventricular systolic and diastolic dysfunction in monocrotalineinduced pulmonary hypertension', Basic research in cardiology, 2009, 104, (5), pp. 535-545

[8] Cerqueira M D, Weissman N J, Dilsizian V, Jacobs A K, Kaul S, Laskey W K, Pennell D J, Rumberger J A, Ryan T J and Verani M S, Standardized myocardial segmentation and nomenclature for tomographic imaging of the heartJ. Cardiovasc. Magn. Reson,.4, pp203–10, 2002

[9] Vasiljevic, J.D., Popovic, Z.B., Otasevic, P., Popovic, Z.V., Vidakovic, R., Miric, M., and Neskovic, A.N.: 'Myocardial fibrosis assessment by semiquantitative, point-counting and computer-based methods in patients with heart muscle disease: a comparative study', Histopathology, 2001, 38, (4), pp. 338-343

[10] M. Gibb, R. Burton, C. Bollensdorff, C. Afonso, T. Mansoori, U. Schotten, D. Gavaghan, B. Rodriguez, J. Schneider, P. Kohl, V. Grau, Resolving the Three-Dimensional Histology of the Heart, Proc. Computational Methods in Systems Biology,2012, pp 2-16

[11] T. Ju, J. Warren, J. Carson, M. Bello, I. Kakadiaris, W. Chiu, C. Thaller,and G. Eichele, "3d volume reconstruction of a mouse brain from histological sections using warp filtering,"Journal of Neuroscience Methods, vol. 156, pp. 84–100, 2006

[12] G. Malandain, E. Bardinet, K. Nelissen, and W. Vanduffel, "Fusion of radiographs with mr volume using 2d and 3d linear transforms,"NeuroImage, vol. 23, pp. 111–127, 2004.

[13] C. Palm ; G. Penney ; W. Crum ; J. Schnabel ; U. Pietrzyk ; D. Hawkes, Fusion of rat brain histology and MRI using weighted multi-image mutual information, Proc. SPIE Medical Imaging, 2008

[14] C. Kuglin and D. Hines, The phase correlation image alignment method, Proc. Int. Conf. Cybern. Soc., 1975, pp. 163–165.

[15] D. Casasent and D. Psaltis, Position, rotation, and scale invariant optical correlation, Appl. Opt., vol. 15, no. 7, pp. 1795–1799, 1976

[16] Song, Y., Treanor D., Bulpitt, A.J., Wijayathunga N., Roberts N., Wilcox R., Magee D., Unsupervised Content Classification Based Non-rigid Registration of Differently Stained Histology Images, IEEE Transactions on Biomedical Engineering,Vol 61(1), 2014

[17] Levenberg, K., A Method for the Solution of Certain Non-Linear Problems in Least Squares, Quarterly of Applied Mathematics 2: 164–168, 1944

Figure 1. Single Stain Reconstruction results (stack views, 1 line per image) (a) Bowel cancer in human liver (50 µm slice spacing, paraffin embedded, H&E stained), (b) Rat Glomorulus (0.5 µm slice spacing, Plastic Embedded, H&E stained)
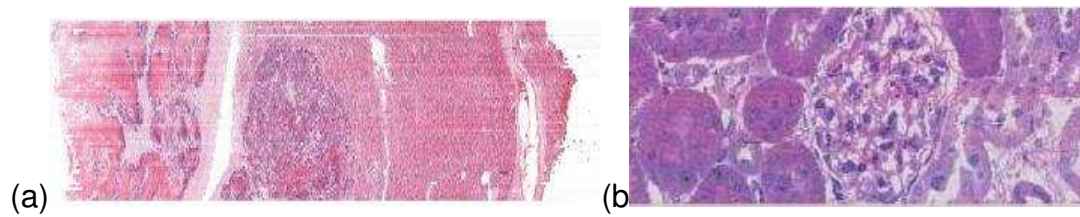

(a)

(b)

Figure 2: Tissue Class Images: (a) Two histopathology images with different stains [left: original images and sub image, right: 3 "tissue class probability images" corresponding to each image/tissue class, (b) Histopathology image and MRI image]
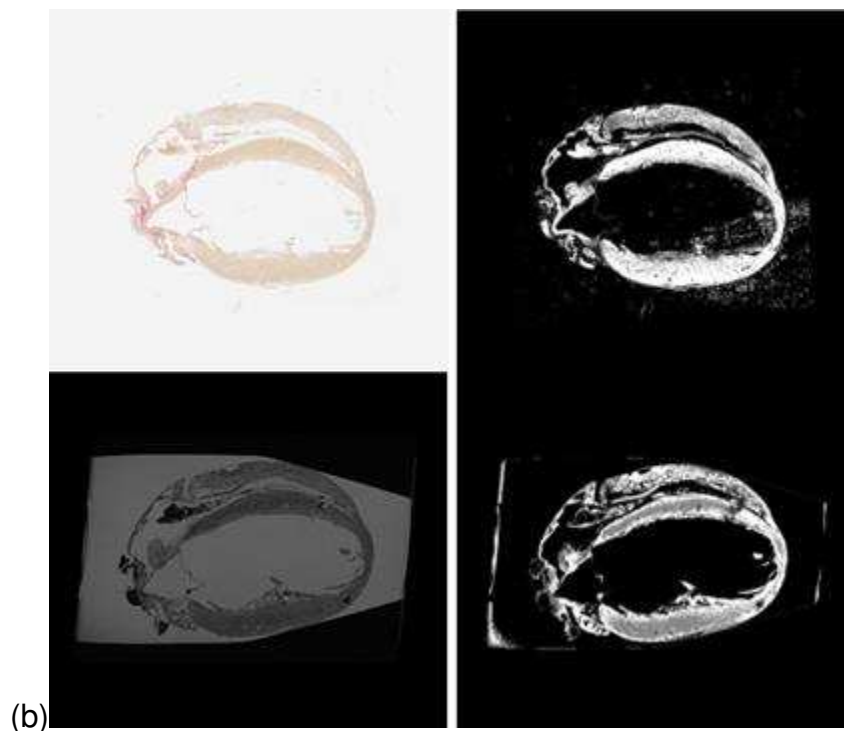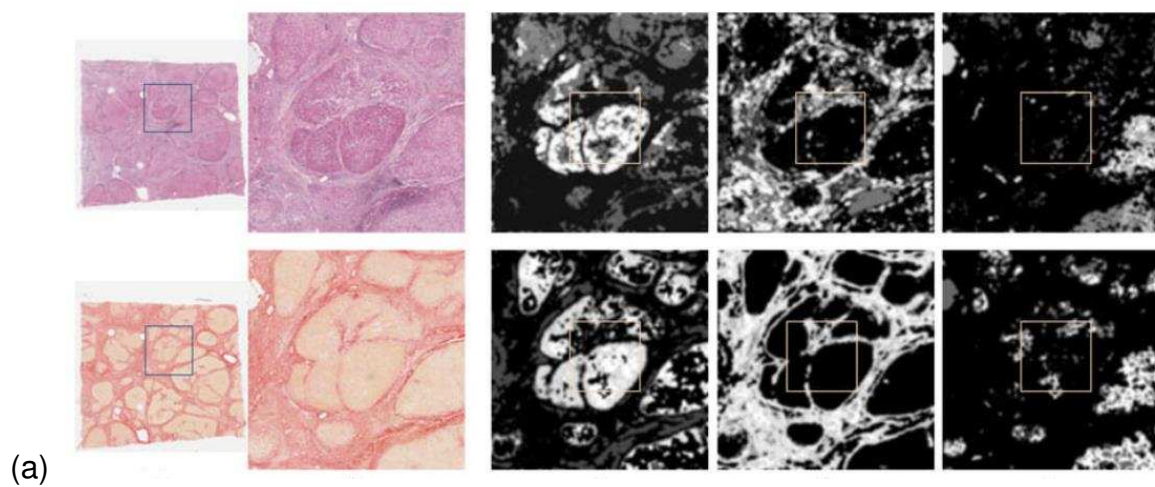

(a)

(b)

Figure 3: Liver tissue Quantification. (a) Left: Original Data, Right: "Stacks View" of reconstructed data (one row from each image). (b) Volume rendering of reconstructed liver tissue
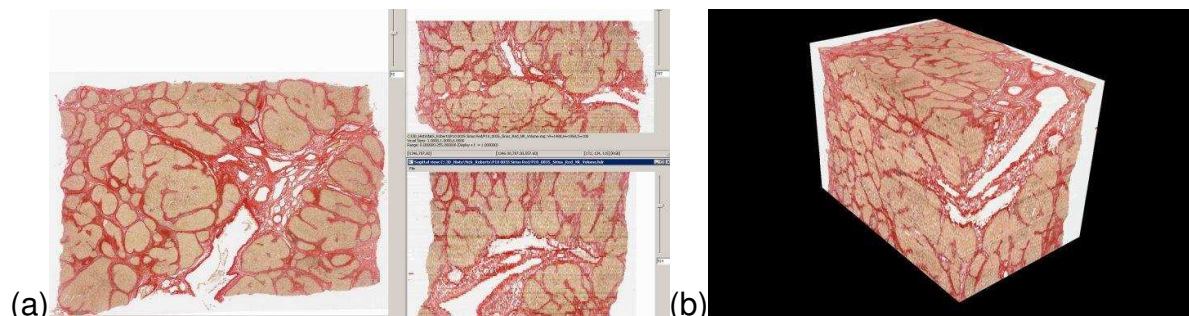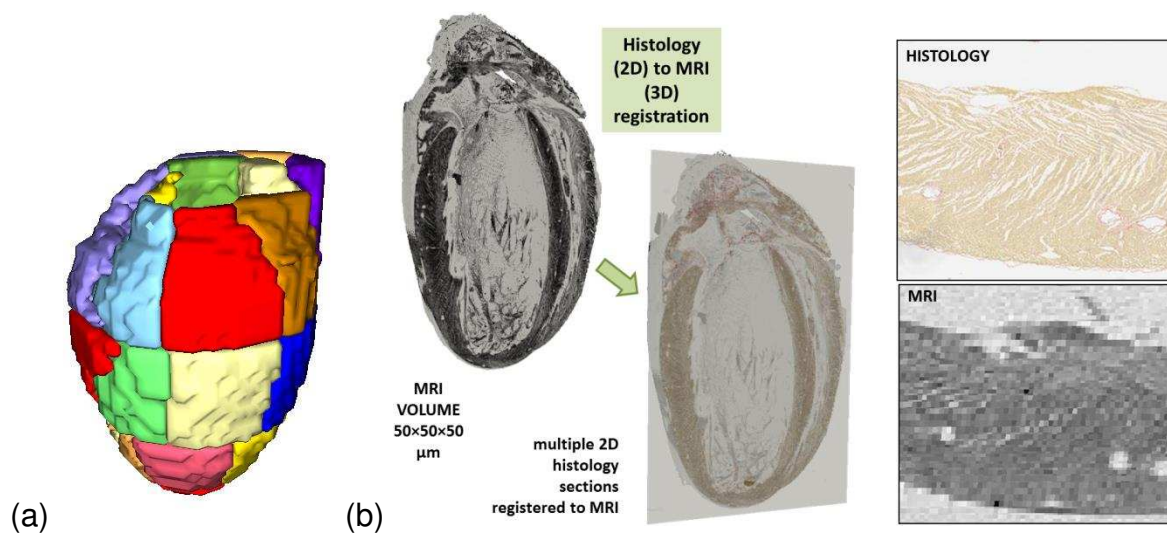

(a)

(b)

Figure 4: Rat Heart Collagen Quantification (a) 3D Segmentation of MRI based on the AHA heart model, (b) Histology to MRI Registration

(a)

(b)

Declaration: Figures 1-3 are "original" in the sense they are generated by the authors of this manuscript.